High-throughput Evaluation of Epilepsy-associated *KCNQ2* Variants Reveals Functional and Pharmacological Heterogeneity

Carlos G. Vanoye, Reshma R. Desai, Zhigang Ji, Sneha Adusumilli, Nirvani Jairam, Nora Ghabra, Nishtha Joshi, Eryn Fitch, Katherine Helbig, Dianalee McKnight, Amanda Lindy, Fanggeng Zou, Ingo Helbig, Edward C. Cooper, and Alfred L. George, Jr.

SUPPLEMENTARY MATERIAL

Supplemental Figures

Fig. S1 KCNQ2 variants analyzed in this study
Fig. S2 Comparison of automated and manual patch clamp recording of KCNQ2/KCNQ3
Fig. S3 Whole-cell currents from literature KCNQ2 variants (homozygous state)
Fig. S4 Whole-cell currents from literature KCNQ2 variants (heterozygous state)
Fig. S5 Manual and automated patch clamp analyses of KCNQ2 variants (heterozygous state)
Fig. S6 Whole-cell currents of KCNQ2 population variants (homozygous state)
Fig. S7 Whole-cell currents of KCNQ2 population variants (heterozygous state)
Fig. S8 Whole-cell currents of KCNQ2 epilepsy variants (homozygous state)
Fig. S9 Whole-cell currents of KCNQ2 epilepsy variants (heterozygous state)
Fig. S10 Retigabine effects on KCNQ2 variants expressed in the homozygous state
Fig. S11 Retigabine effects on KCNQ2 variants expressed in the heterozygous state

Supplemental Tables

Table S1 KCNQ2 variant information
Table S2 Sequence of mutagenic primers used to generate KCNQ2 variants
Table S3 Data from manual and automated patch clamp recording of KCNQ2 in CHO-Q3 cells
Table S4 Functional properties of homozygous KCNQ2 variants under control conditions
Table S5 Functional properties of heterozygous KCNQ2 variants under control conditions
Table S6 Functional properties of homozygous KCNQ2 variants after exposure to retigabine
Table S7 Functional properties of heterozygous KCNQ2 variants after exposure to retigabine

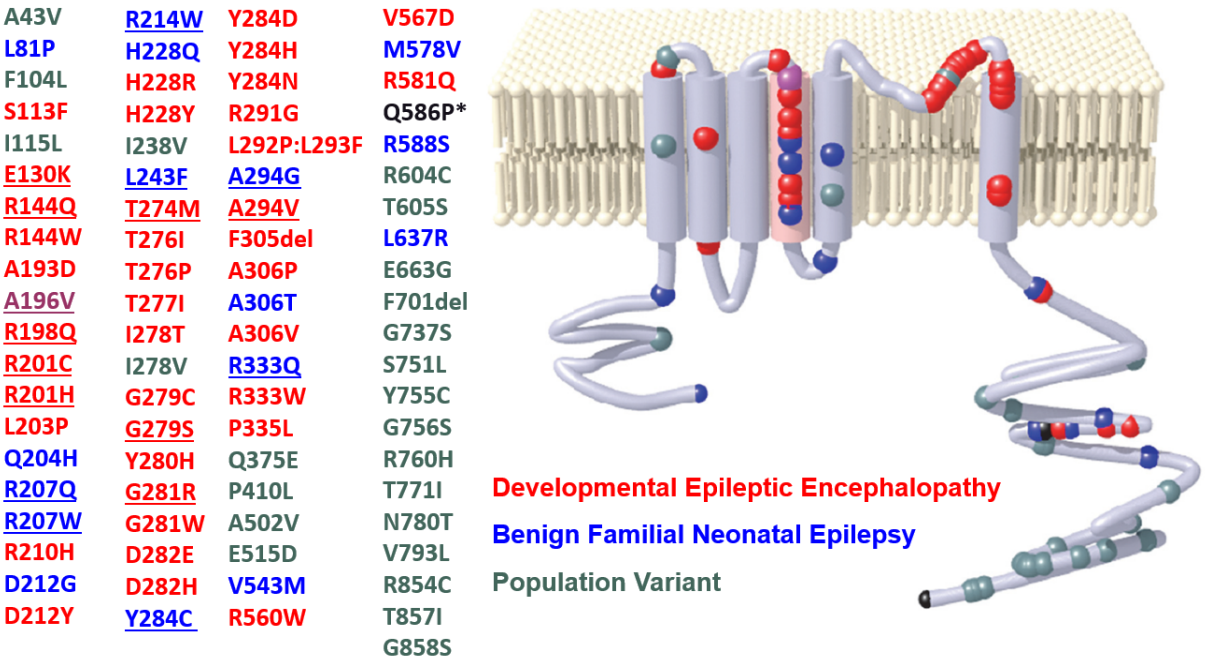

Figure S1. KCNQ2 variants analyzed in this study. Location and classification of the 81 KCNQ2 variants analyzed in this study. BFNE-associated variants are shown as blue dots, DEE-associated variants as red dots, the purple dot represents a variant associated with both BFNE and DEE, and population variants are denoted as green dots. Variant Q586P (marked by *) is associated with unknown phenotype category. Literature variants are underlined.

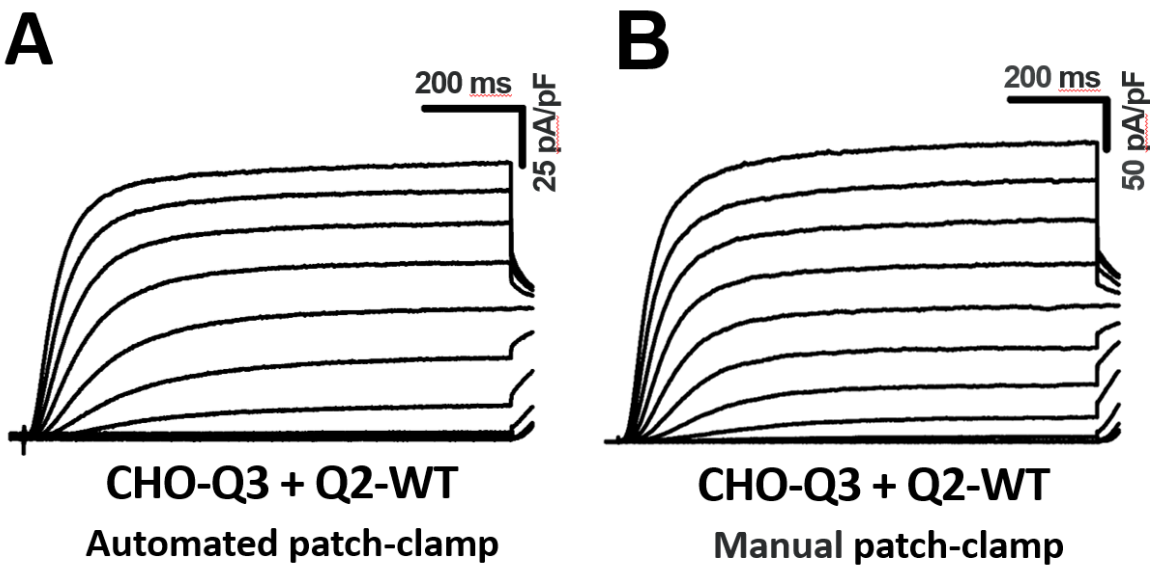

Figure S2. Comparison of automated and manual patch clamp recording of KCNQ2/KCNQ3. Whole cell current density recorded from CHO-Q3 cells electroporated with wild type KCNQ2 (Q2-WT) using either automated (**A**) or manual (**B**) patch clamp.

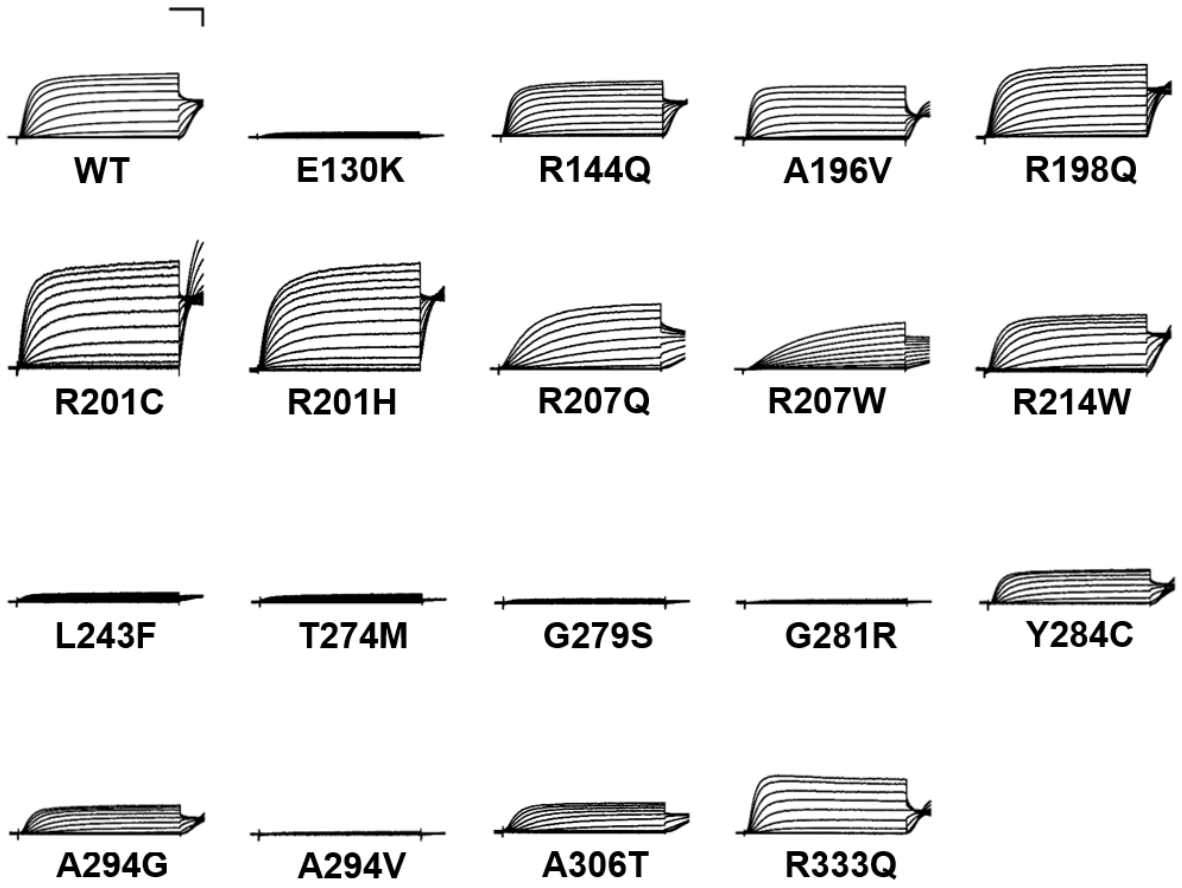

Figure S3. Whole-cell currents from literature KCNQ2 variants expressed as homozygous channels. Average XE-991-sensitive whole-cell currents recorded by automated patch clamp from CHO-Q3 cells electroporated with KCNQ2 variants from the literature set and normalized to wild type channel peak current recorded in parallel. For variant R201C, whole-cell currents were recorded from CHO-K1 cells co-electroporated with KCNQ3-WT plus KCNQ2-variant. Scale bars are 200 ms (horizontal) and 25% of WT channel current density (vertical).

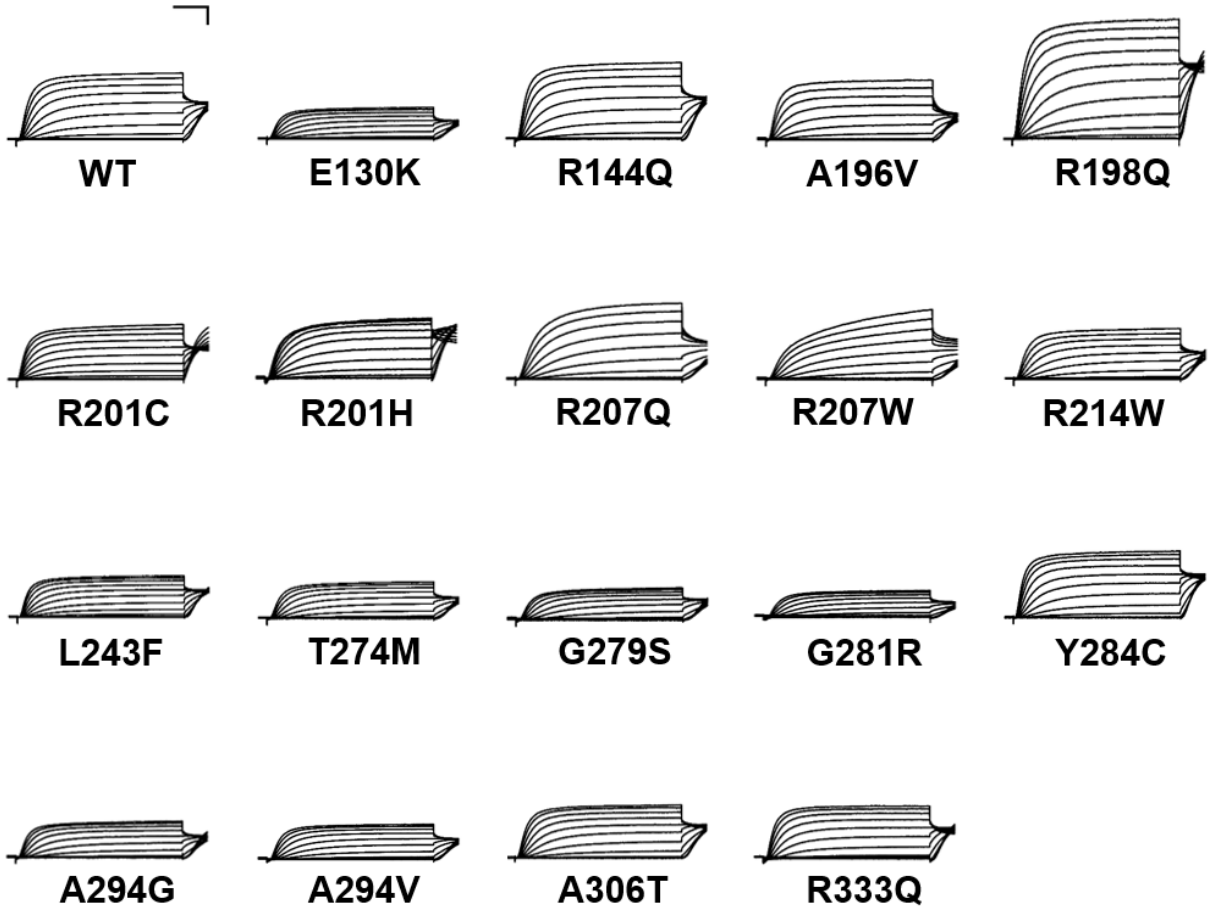

Figure S4. Whole-cell currents from literature KCNQ2 variants expressed as heterozygous channels. Average XE-991-sensitive whole-cell currents recorded by automated patch clamp from CHO-Q3 cells co-electroporated with wild type plus variant KCNQ2 cDNA from the literature set and normalized to wild type channel peak current recorded in parallel. Scale bars are 200 ms (horizontal) and 25% of WT channel current density (vertical).

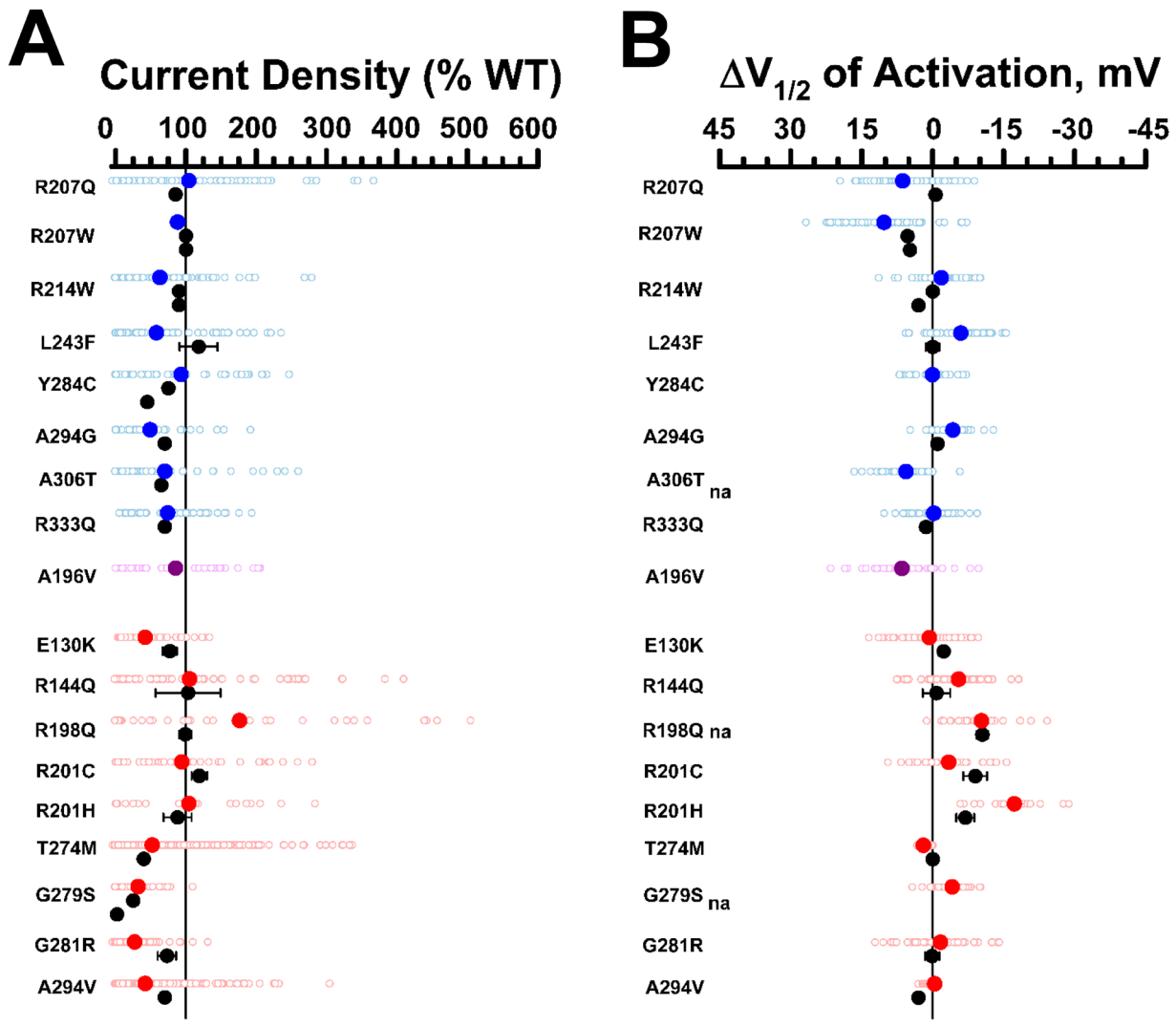

Figure S5. Manual and automated voltage clamp analyses of KCNQ2 variants expressed in the heterozygous state yield similar biophysical properties. A. Average whole-cell currents recorded at +40 mV from CHO-Q3 cells co-expressing variant + wild type KCNQ2 and normalized to WT channel peak current that was measured in parallel. **B**. Change (△) in voltage-dependence of activation V½ determined for heterozygous KCNQ2 variants relative to the WT channel △V½ measured in parallel. Black symbols represent mean ± SEM voltage-clamp data from literature reported variants (error bars are smaller than data symbol in some cases), while automated patch clamp results are shown as blue for BFNE, red for DEE, or purple symbols for BFNE/DEE pathogenic variants. All experimental data are presented as open circles with filled circles representing mean values. na = not available in the literature.

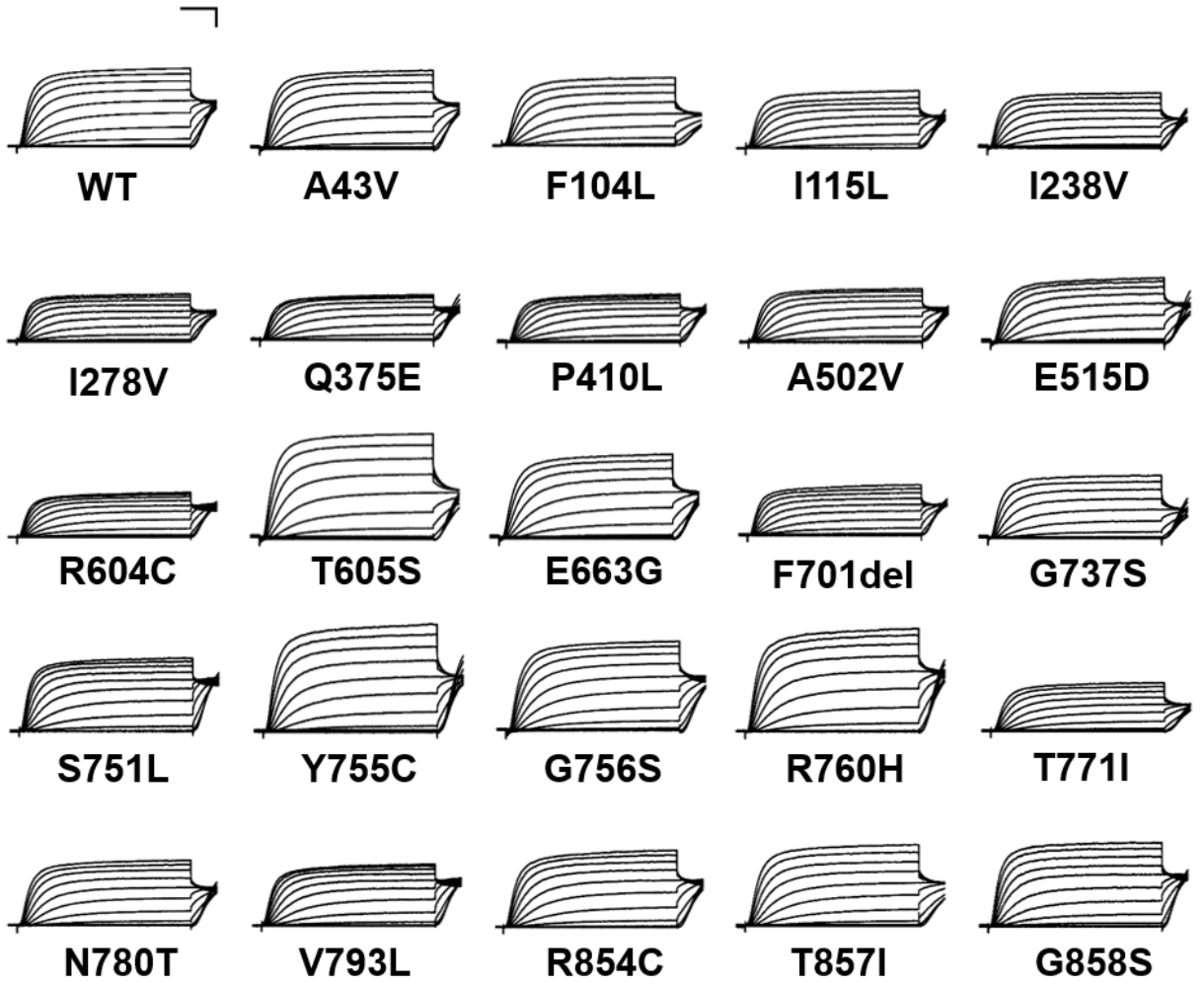

Figure S6. Average whole-cell currents recorded from CHO-Q3 cells electroporated with population KCNQ2 variants. Average XE-991-sensitive whole-cell currents recorded by automated patch clamp from CHO-Q3 cells electroporated with rare population KCNQ2 variants and normalized to wild type channel peak current measured in parallel. Scale bars are 200 ms (horizontal) and 25% of WT channel current density (vertical).

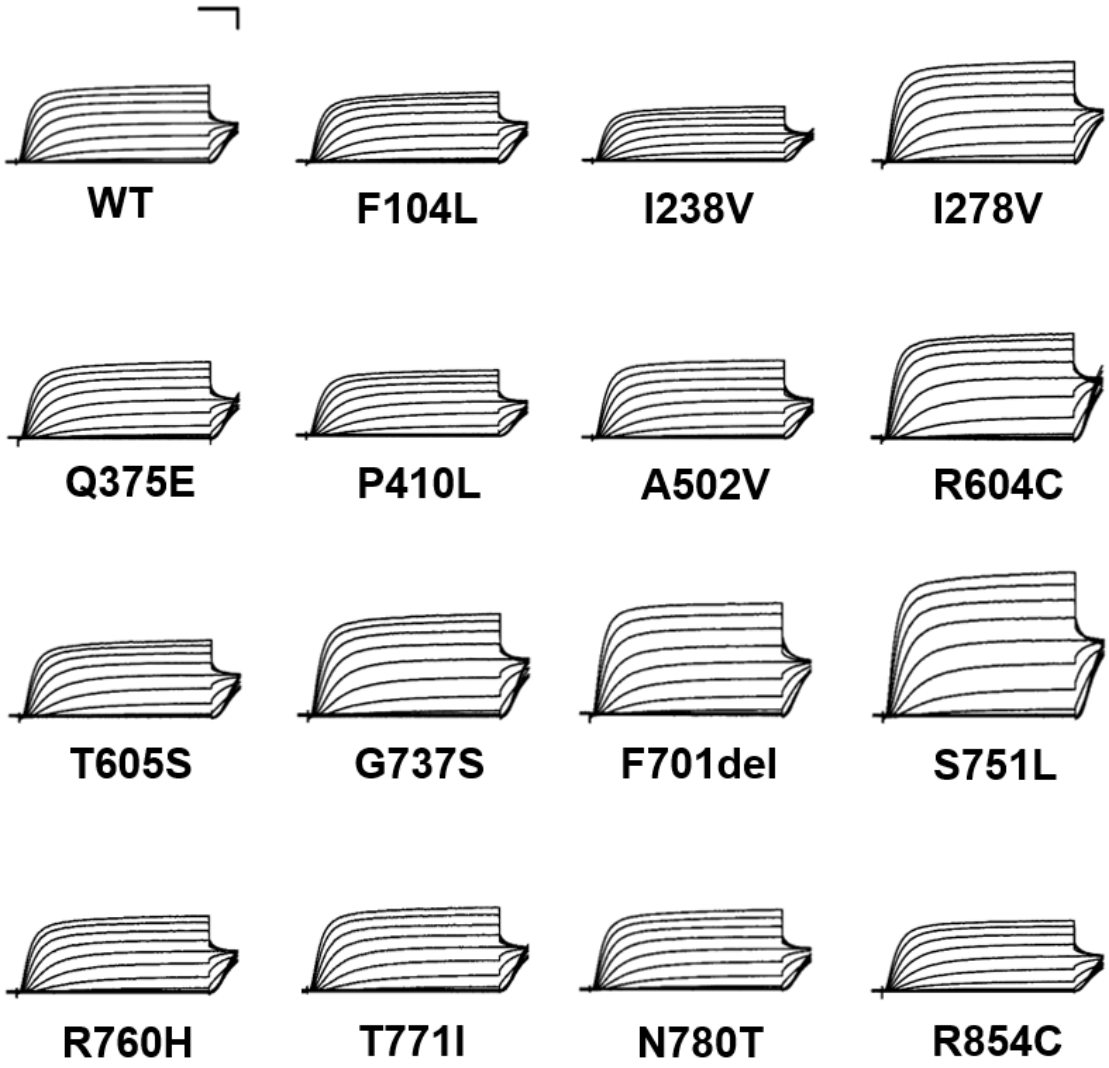

Figure S7. Average whole-cell currents recorded from CHO-Q3 cells co-electroporated with selected population variants plus wild type KCNQ2. Average XE-991-sensitive whole-cell currents recorded by automated patch clamp from CHO-Q3 cells co-electroporated with rare population variants plus wild type KCNQ2 and normalized to wild type channel peak current recorded in parallel. Scale bars are 200 ms (horizontal) and 25% of WT channel current density (vertical).

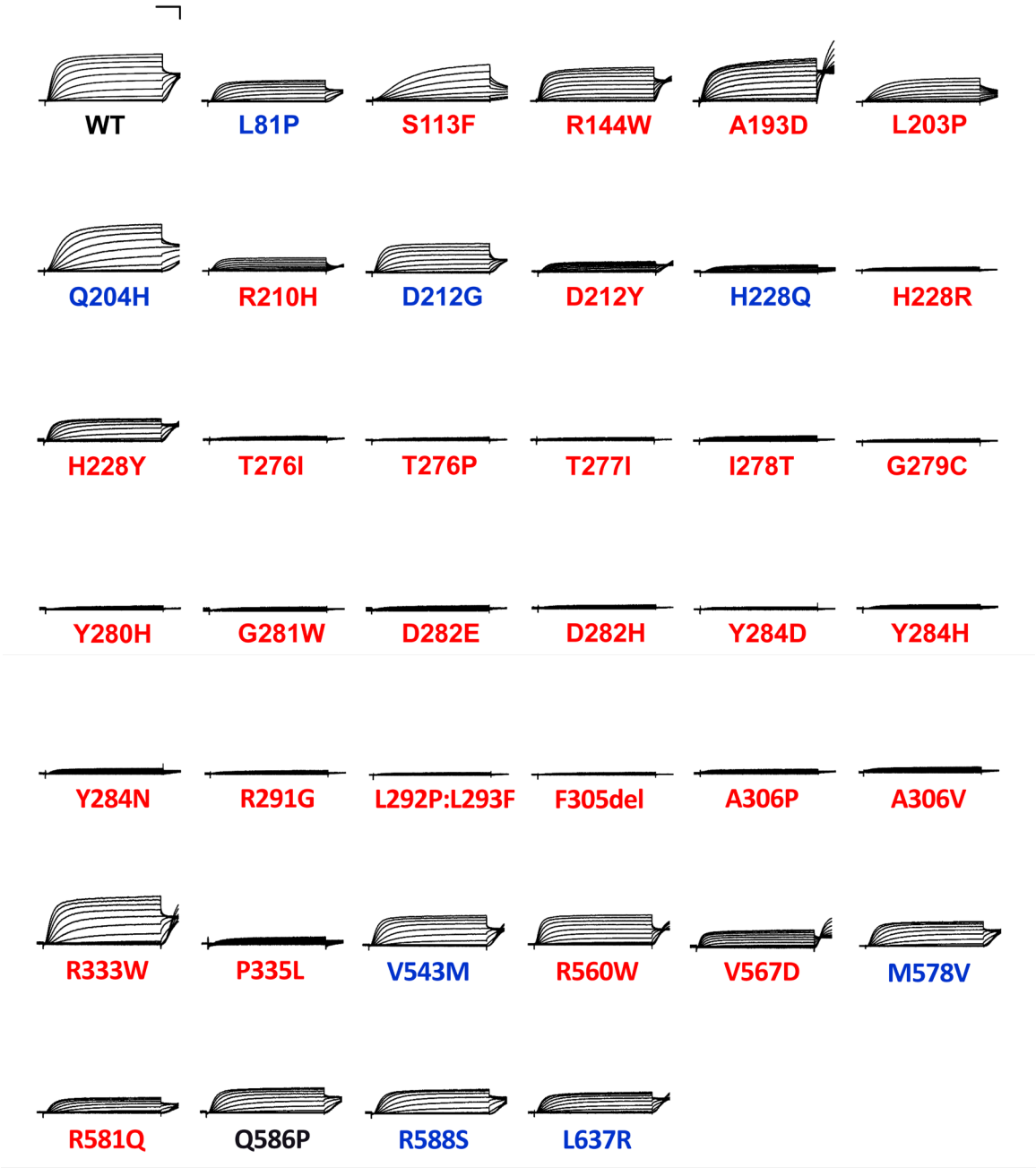

Figure S8. Whole-cell currents from epilepsy-associated KCNQ2 variants expressed as homozygous channels. Average XE-991-sensitive whole-cell currents recorded by automated patch clamp from CHO-Q3 cells electroporated with epilepsy-associated KCNQ2 variants and normalized to wild type channel peak current recorded in parallel. Variant labels: **Blue** = BFNE-associated; **Red** = DEE-associated; **Black** = unknown phenotype category (Q586P). For A193D and P335L, whole-cell currents were recorded from CHO-K1 cells co-electroporated with KCNQ3-WT plus KCNQ2-variant. Scale bars are 200 ms (horizontal) and 25% of WT channel current density (vertical).

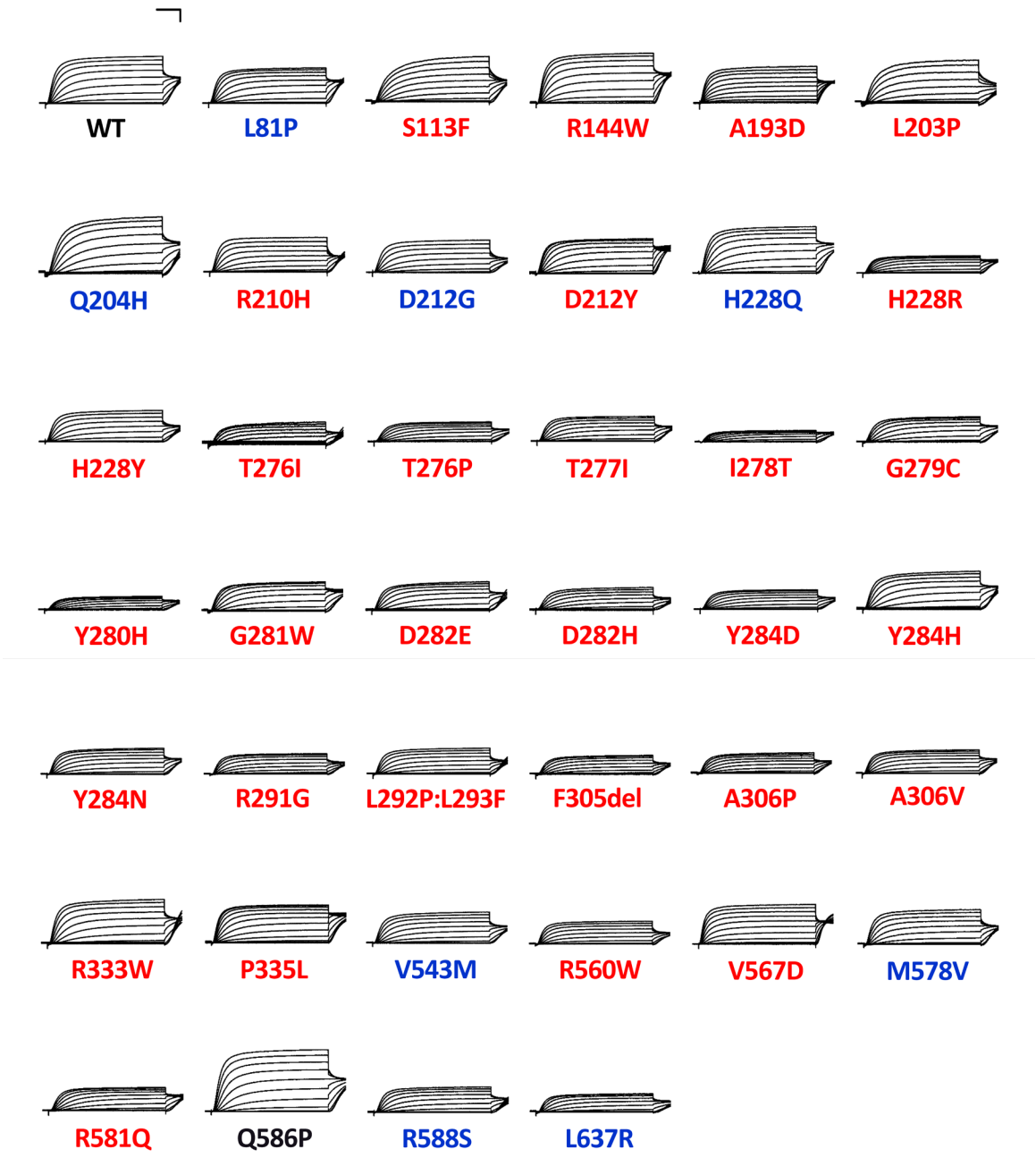

Figure S9. Average whole-cell currents recorded from CHO-Q3 cells co-electroporated with epilepsy-associated variants plus wild type KCNQ2. Average XE-991-sensitive whole-cell currents recorded by automated patch clamp from CHO-Q3 cells co-electroporated with epilepsy-associated KCNQ2 variants plus WT KCNQ2 and normalized to wild type channel peak current recorded in parallel. Variant labels: **Blue** = BFNE-associated; **Red** = DEE-associated; **Black** = unknown phenotype category (Q586P). Scale bars are 200 ms (horizontal) and 25% of WT channel current density (vertical).

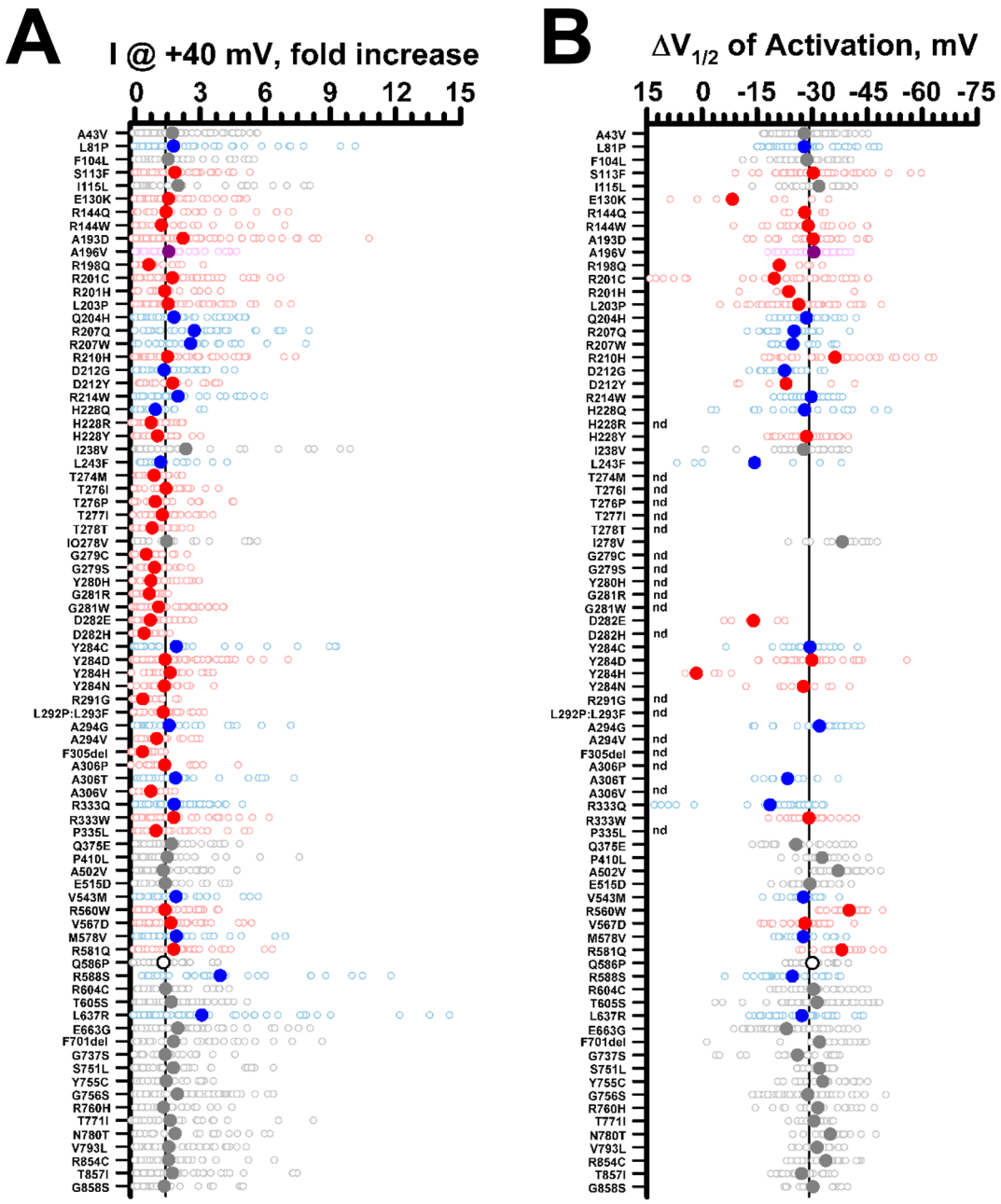

Figure S10. Retigabine effects on whole-cell currents recorded from KCNQ2 variants expressed in the homozygous state. A) Ratio of whole-cell currents recorded at +40 mV after exposure to 10 μM retigabine and divided by the current measured under control conditions (n = 15-86). **B**) Change in voltage-dependence of activation V½ determined for whole-cell currents after exposure to 10 μM retigabine (n = 5-74). Dashed lines indicate average effect of retigabine on current amplitude and change in voltage-dependence of activation V½ in the wild type channel. All experimental data are presented as open circles with larger filled circles representing mean values for BFNE (blue), DEE (red), BFNE/DEE (purple), unclear phenotype (white) or population (grey) variants. For complete list of results, see **Supplemental Table 6**.

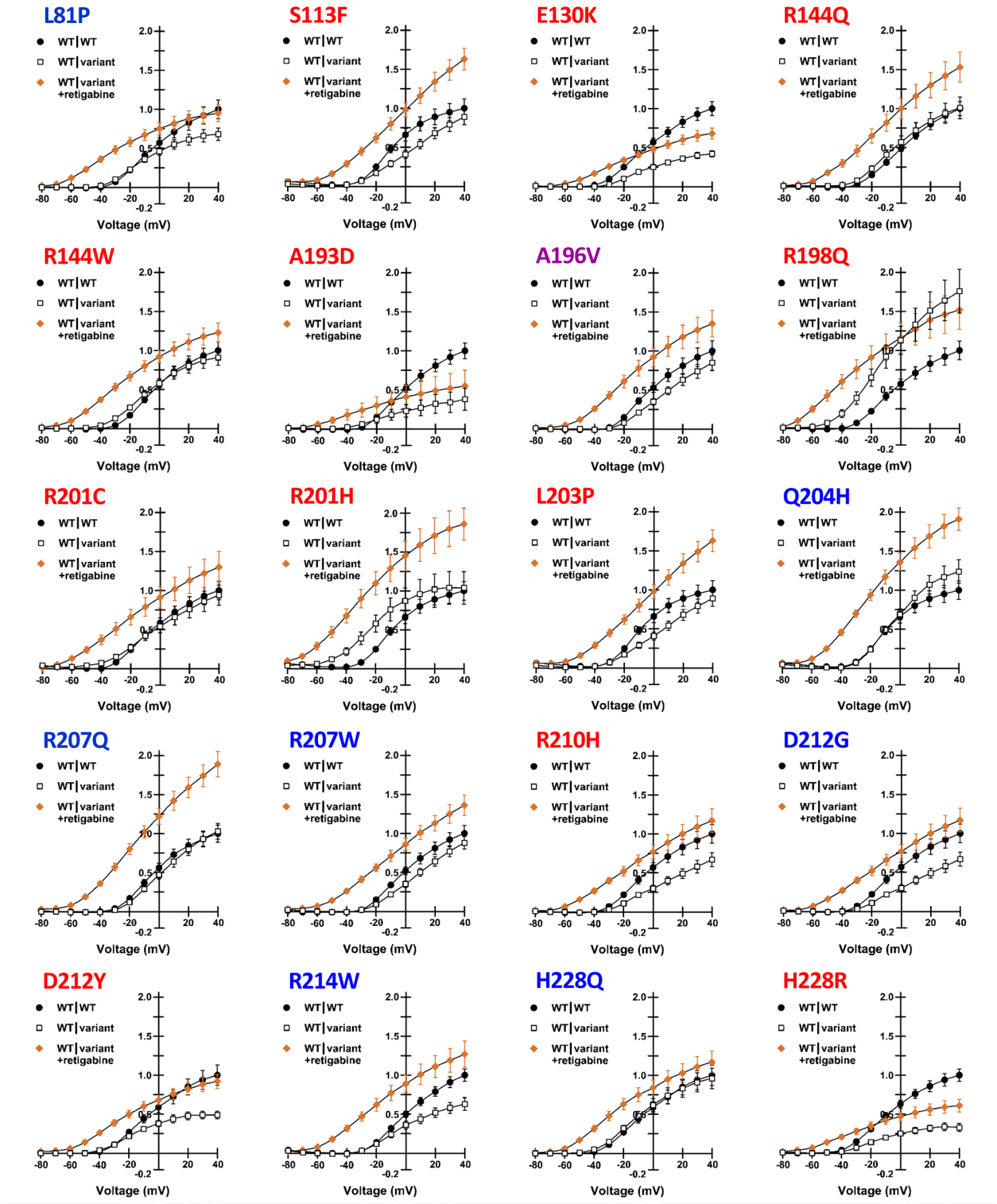

Figure S11. Retigabine effects on whole-cell currents recorded from epilepsy-associated KCNQ2 variants expressed in the heterozygous state. Normalized current-voltage relationships for each variant expressed in the heterozygous state recorded in the absence of retigabine (WT|variant, open squares) compared with heterozygous variants recorded in the absence of retigabine (WT|variant +retigabine, orange filled diamonds). Currents were first normalized to cell capacitance, then re-normalized to the peak current for WT channels recorded in parallel (WT|WT, filled circles). Variant labels: **Blue** = BFNE-associated; **Red** = DEE-associated; **Purple** = BFNE/DEE; **Black** = unknown phenotype category. Complete data sets are presented in **Table S7**.

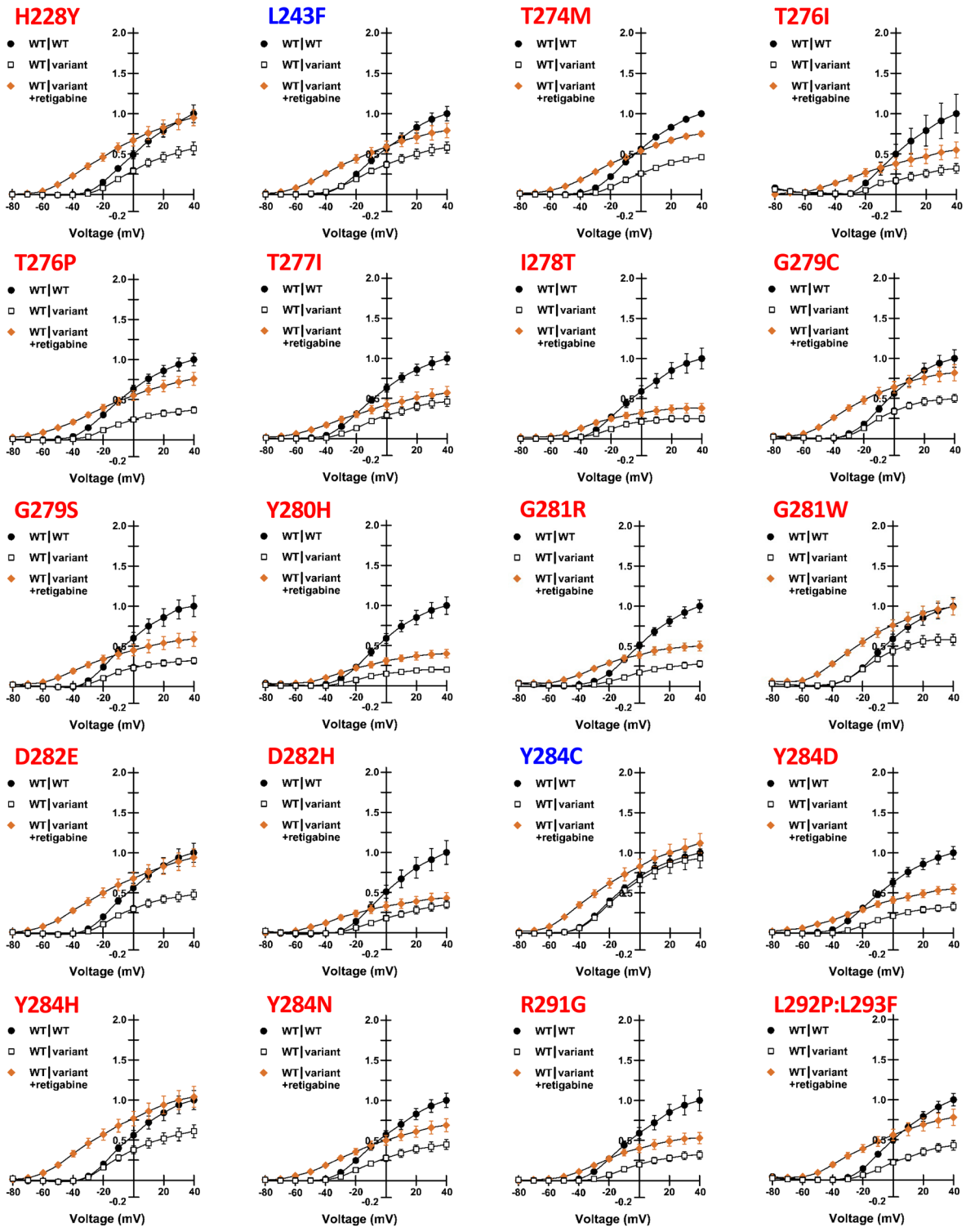

Figure S11 - *continued*. **Retigabine effects on whole-cell currents recorded from epilepsy-associated KCNQ2 variants expressed in the heterozygous state.** Normalized current-voltage relationships for each variant expressed in the heterozygous state recorded in the absence of retigabine (WT|variant, open squares) compared with heterozygous variants recorded in the absence of retigabine (WT|variant +retigabine, orange filled diamonds). Currents were first normalized to cell capacitance, then re-normalized to the peak current for WT channels recorded in parallel (WT|WT, filled circles). Variant labels: **Blue** = BFNE-associated; **Red** = DEE-associated; **Purple** = BFNE/DEE; **Black** = unknown phenotype category. Complete data sets are presented in **Table S7**.

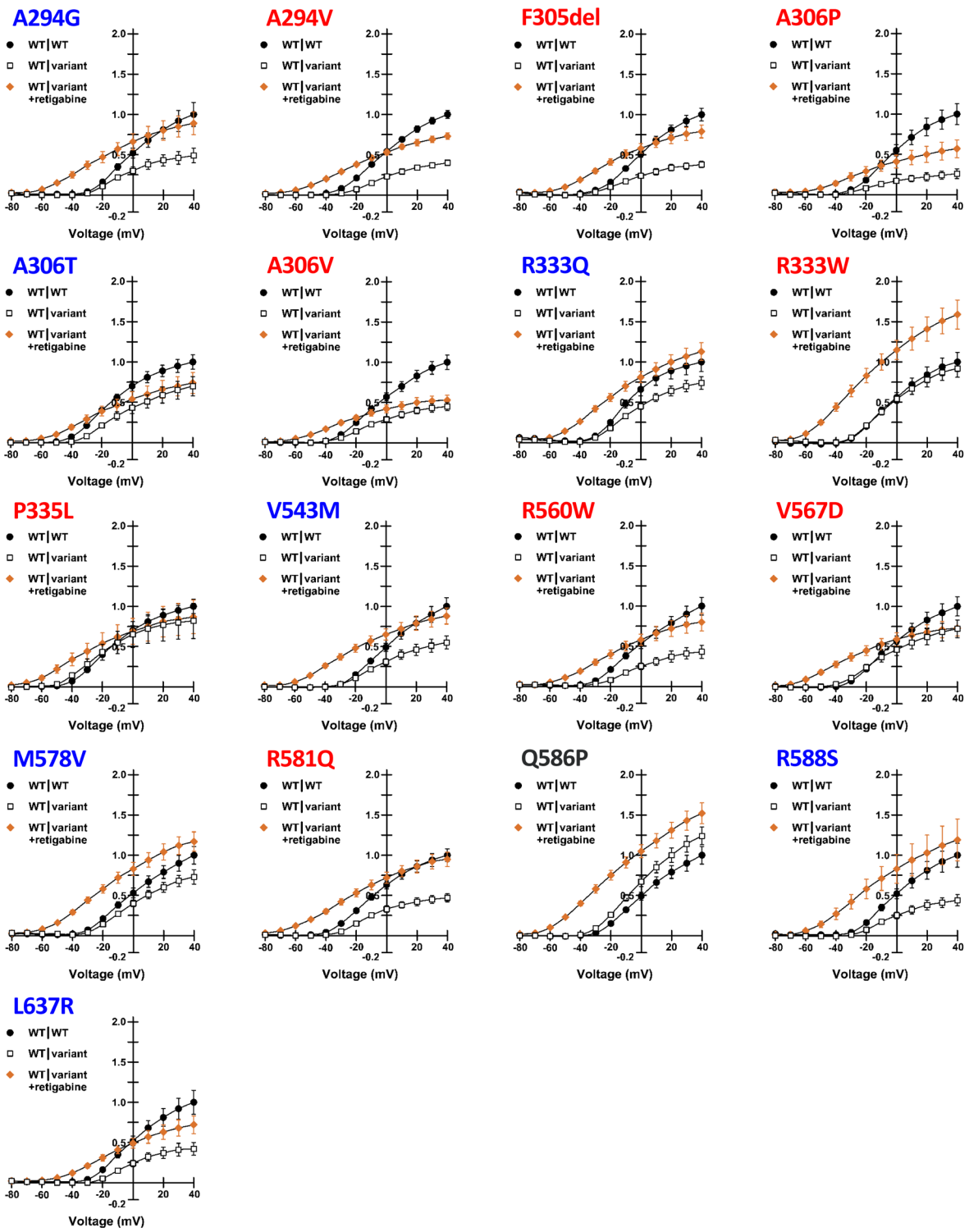

Figure S11 - *continued*. **Retigabine effects on whole-cell currents recorded from epilepsy-associated KCNQ2 variants expressed in the heterozygous state.** Normalized current-voltage relationships for each variant expressed in the heterozygous state recorded in the absence of retigabine (WT|variant, open squares) compared with heterozygous variants recorded in the absence of retigabine (WT|variant +retigabine, orange filled diamonds). Currents were first normalized to cell capacitance, then re-normalized to the peak current for WT channels recorded in parallel (WT|WT, filled circles). Variant labels: **Blue** = BFNE-associated; **Red** = DEE-associated; **Purple** = BFNE/DEE; **Black** = unknown phenotype category. Complete data sets are presented in **Table S7**.

Table S1 – KCNQ2 variant information

Nucleotide	Amino Acid	Channel Domain	Phenotype	MAF (gnomAD)	ClinVar	PubMed ID
c.128C>T	p.Ala43Val	N-term	PV	0.000176	LB/VUS	
c.242T>C	p.Leu81Pro	N-term	BFNE	0	N/A	29215089
c.312C>G	p.Phe104Leu	TMD: S1	PV	0.000008	N/A	
c.338C>T	p.Ser113Phe	TMD: S1-S2-Link	DEE	0	VUS/LP	29655203
c.343A>C	p.Ile115Leu	TMD: S1-S2-Link	PV	0.000016	N/A	
c.388G>A	p.Glu130Lys	TMD: S2	DEE	0	PATH	27535030
c.431G>A	p.Arg144Gln	TMD: S2-S3-Link	DEE	0	PATH/LP	23934111
c.430C>T	p.Arg144Trp	TMD: S2-S3-Link	DEE	0	PATH/LP	28628100; 28867141
c.578C>A	p.Ala193Asp	TMD: S2-S3-Link	DEE	0	PATH	27602407
c.587C>T	p.Ala196Val	TMD: S4	DEE	0	PATH	17475800
c.593G>A	p.Arg198Gln	TMD: S4	DEE	0	PATH	27861786
c.601C>T	p.Arg201Cys	TMD: S4	DEE	0	PATH/VUS	24107868
c.602G>A	p.Arg201His	TMD: S4	DEE	0	PATH	23708187
c.608T>C	p.Leu203Pro	TMD: S4	DEE	0	PATH	26007637
c.612G>T	p.Gln204His	TMD: S4	BFNE	0	LP	27602407
c.620G>A	p.Arg207Gln	TMD: S4	DEE	0	PATH/LP	17872363
c.619C>T	p.Arg207Trp	TMD: S4	BFNE	0	PATH	11572947
c.629G>A	p.Arg210His	TMD: S4	DEE	0	PATH	24107868
c.635A>G	p.Asp212Gly	TMD: S4	BFNE	0	N/A	19344764
c.634G>T	p.Asp212Tyr	TMD: S4	DEE	0	PATH	28817111
c.640C>T	p.Arg214Trp	TMD: S4	BFNE	0	PATH/LP	11175290; 29056246
c.684C>A	p.His228Gln	TMD: S4-S5-Link	BFNE	0	VUS	14534157
c.683A>G	p.His228Arg	TMD: S4-S5-Link	DEE	0	LP	
c.682C>T	p.His228Tyr	TMD: S4-S5-Link	BFNE	0	Not Provided	28837158
c.712A>G	p.Ile238Val	TMD: S5	PV	0.000008	VUS	
c.727C>T	p.Leu243Phe	TMD: S5	BFNE	0	PATH	14534157
c.821C>T	p.Thr274Met	TMD: P-loop	DEE	0	PATH	22275249
c.827C>T	p.Thr276Ile	TMD: P-loop	DEE	0	PATH	24463883
c.826A>C	p.Thr276Pro	TMD: P-loop	DEE	0	N/A	29720203
c.830C>T	p.Thr277Ile	TMD: P-loop	DEE	0	N/A	26544041
c.833T>C	p.Ile278Thr	TMD: P-loop	DEE	0	LP	30109124
c.832A>G	p.Ile278Val	TMD: P-loop	PV	0.000008	N/A	
c.835G>T	p.Gly279Cys	TMD: P-loop	DEE	0	PATH	25959266
c.836G>A	p.Gly279Ser	TMD: P-loop	DEE	0	N/A	27734276
c.838T>C	p.Tyr280His	TMD: P-loop	DEE	0	PATH	27779742
c.841G>A	p.Gly281Arg	TMD: P-loop	DEE	0	LP	24107868
c.841G>T	p.Gly281Trp	TMD: P-loop	DEE	0	PATH	25880994
c.846C>A	p.Asp282Glu	TMD: P-loop	DEE	0	N/A	28133863
c.844G>C	p.Asp282His	TMD: P-loop	DEE	0	VUS/LP	29655203
c.851A>G	p.Tyr284Cys	TMD: P-loop	BFNE	0	PATH	9425895
c.850T>G	p.Tyr284Asp	TMD: P-loop	DEE	0	PATH	27535030
c.850T>C	p.Tyr284His	TMD: P-loop	DEE	0	N/A	29588952
c.850T>A	p.Tyr284Asn	TMD: P-loop	DEE	0	N/A	
c.871A>G	p.Arg291Gly	TMD: P-loop	DEE	0	N/A	27779742
c.[875T>C:877C>T]	p.Leu292Pro:Leu293Phe	TMD: S6	DEE	0	LP , VUS	

Table S1 – *(continued)* KCNQ2 variant information

Nucleotide	Amino Acid	Channel Domain	Phenotype	MAF (gnomAD)	ClinVar	PubMed ID
c.881C>G	p.Ala294Gly	TMD: S6	BFNE	0	PATH	17129708
c.881C>T	p.Ala294Val	TMD: S6	DEE	0	PATH	17129708
c.913_915delTTC	p.Phe305del	TMD: S6	DEE	0	N/A	28554332; 28728838; 18640800
c.916G>C	p.Ala306Pro	TMD: S6	DEE	0	PATH	29655203
c.916G>A	p.Ala306Thr	TMD: S6	DEE	0	PATH	9425895; 26138355
c.917C>T	p.Ala306Val	TMD: S6	DEE	0	PATH	31152295
c.998G>A	p.Arg333Gln	C-term	BFNE	0.000004	PATH/LP	29215089; 14534157
c.997C>T	p.Arg333Trp	C-term	DEE	0	PATH	16039833
c.1004C>T	p.Pro335Leu	C-term	DEE	0	PATH/LP	28867141
c.1123C>G	p.Gln375Glu	C-term	DEE	0.000018	N/A	
c.1229C>T	p.Pro410Leu	C-term	PV	0.000043	VUS	
c.1505C>T	p.Ala502Val	C-term	PV	0.000036	VUS	
c.1545G>C	p.Glu515Asp	C-term	PV	0.002517	B/LB/VUS	19380078
c.1627G>A	p.Val543Met	C-term	BFNE	0.000004	VUS/LP	28399683
c.1678C>T	p.Arg560Trp	C-term	DEE	0	PATH/LP	22275249
c.1700T>A	p.Val567Asp	C-term	DEE	0	LP	27888506
c.1732A>G	p.Met578Val	C-term	BFNE	0	PATH/LP	25982755
c.1742G>A	p.Arg581Gln	C-term	DEE	0	PATH/LP	27864847
c.1757A>C	p.Gln586Pro	C-term	DEE	0	VUS	
c.1764A>T	p.Arg588Ser	C-term	BFNE	0	PATH	25982755
c.1810C>T	p.Arg604Cys	C-term	PV	0.000008	VUS	
c.1814C>G	p.Thr605Ser	C-term	PV	0.000056	VUS/LB	
c.1910T>G	p.Leu637Arg	C-term	BFNE	0	PATH	25982755
c.1988A>G	p.Glu663Gly	C-term	PV	0.000047	N/A	
c.2101_2103delTCT	p.Phe701del	C-term	PV	0.000009	N/A	
c.2209G>A	p.Gly737Ser	C-term	PV	0.000016	VUS	
c.2252C>T	p.Ser751Leu	C-term	PV	0.000065	VUS	
c.2264A>G	p.Tyr755Cys	C-term	PV	0.002953	B/LB	
c.2266G>A	p.Gly756Ser	C-term	PV	0.000264	LB	
c.2279G>A	p.Arg760His	C-term	PV	0.000059	VUS	
c.2312C>T	p.Thr771Ile	C-term	PV	0.000047	VUS	
c.2339A>C	p.Asn780Thr	C-term	PV	0.609194	B	
c.2377G>C	p.Val793Leu	C-term	PV	0.000025	VUS	
c.2560C>T	p.Arg854Cys	C-term	PV	0.000226	B/LB	
c.2570C>T	p.Thr857Ile	C-term	PV	0.000019	N/A	
c.2572G>A	p.Gly858Ser	C-term	PV	0.000030	VUS	

Table S2. Sequence of mutagenic primers used to generate KCNQ2 variants.

Nucleotide change	Amino acid change	Forward Primer	Reverse Primer
c.128C>T	p.Ala43Val	GCTGATCG**T**CGGCTCCGAGGCCCCCAAG	CGGAGCCG**A**CGATCAGCAGCGCCCCGTCC
c.242T>C	p.Leu81Pro	GCAGAATTTCC**C**CTACAACGTGCTGGAGCGGCC	TGTAG**G**GGAAATTCTGCAGCTTGCGGTAGAAGG
c.312C>G	p.Phe104Leu	CTGGTTTT**G**TCCTGCCTCGTGCTGTCTGTGTTTTC	AGGCAGGA**C**AAAACCAGGAGGAACACGTAGGCGTG
c.338C>T	p.Ser113Phe	GTGTTTT**T**CACCATCAAGGAGTATGAGAAGAGCTCG	TTGATGGTG**A**AAAACACAGACAGCACGAGGCAGGAG
c.343A>C	p.Ile115Leu	TTCCACC**C**TCAAGGAGTATGAGAAGAGCTCGGAGG	ACTCCTTGA**G**GGTGGAAAACACAGACAGCACGAGG
c.388G>A	p.Glu130Lys	CCTG**A**AAATCGTGACTATCGTGGTGTTTGGCGTG	TAGTCACGATTT**T**CAGGATGTAGAGGGCCCCCTC
c.430C>T	p.Arg144Trp	GTACTTCGTG**T**GGATCTGGGCCGCAGGCTGC	AGATCC**A**CACGAAGTACTCCACGCCAAACACC
c.431G>A	p.Arg144Gln	TACTTCGTGC**A**GATCTGGGCCGCAGGCTGCTG	CAGATC**T**GCACGAAGTACTCCACGCCAAACAC
c.578C>A	p.Ala193Asp	CGTCTTTG**A**CACATCTGCGCTCCGGAGCCT	CAGATGTG**T**CAAAGACGTTGCCCTGGGAGCC
c.587C>T	p.Ala196Val	GCCACATCTG**T**GCTCCGGAGCCTGCGCTTCC	CGGAGC**A**CAGATGTGGCAAAGACGTTGCCCTG
c.593G>A	p.Arg198Gln	TCTGCGCTCC**A**GAGCCTGCGCTTCCTGCAGAT	CGCAGGCTC**T**GGAGCGCAGATGTGGCAAAGAC
c.601C>T	p.Arg201Cys	GCCTG**T**GCTTCCTGCAGATTCTGCGGATGATC	CTGCAGGAAGC**A**CAGGCTCCGGAGCGCAGATGT
c.602G>A	p.Arg201His	CCTGC**A**CTTCCTGCAGATTCTGCGGATGATCC	TCTGCAGGAAG**T**GCAGGCTCCGGAGCGCAGATG
c.608T>C	p.Leu203Pro	CTTCC**C**GCAGATTCTGCGGATGATCCGCATG	GCAGAATCTGC**G**GGAAGCGCAGGCTCCGGAGC
c.612G>T	p.Gln204His	CCTGCA**T**ATTCTGCGGATGATCCGCATGGACC	TCCGCAGAAT**A**TGCAGGAAGCGCAGGCTCCGG
c.620G>A	p.Arg207Gln	AGATTCTGC**A**GATGATCCGCATGGACCGGCG	GATCATC**T**GCAGAATCTGCAGGAAGCGCAGG
c.619C>T	p.Arg207Trp	CAGATTCTG**T**GGATGATCCGCATGGACCGGC	ATCATCC**A**CAGAATCTGCAGGAAGCGCAGGC
c.629G>A	p.Arg210His	GCGGATGATCC**A**CATGGACCGGCGGGGAGGC	CCATG**T**GGATCATCCGCAGAATCTGCAGGAAG
c.635A>G	p.Asp212Gly	GATCCGCATGG**G**CCGGCGGGGAGGCACCTG	GCCGG**C**CCATGCGGATCATCCGCAGAATCTG
c.634G>T	p.Asp212Tyr	TGATCCGCATG**T**ACCGGCGGGGAGGCACCTG	CCGGT**A**CATGCGGATCATCCGCAGAATCTGC
c.640C>T	p.Arg214Trp	TGGACCGG**T**GGGGAGGCACCTGGAAGCTGC	GCCTCCCC**A**CCGGTCCATGCGGATCATCCG
c.684C>A	p.His228Gln	TATGCCCA**A**AGCAAGGAGCTGGTCACTGCCTG	TCCTTGCT**T**TGGGCATAGACCACAGAGCCCAG
c.683A>G	p.His228Arg	CTATGCCC**G**CAGCAAGGAGCTGGTCACTGCC	CCTTGCTG**C**GGGCATAGACCACAGAGCCCAG
c.682C>T	p.His228Tyr	CTATGCC**T**ACAGCAAGGAGCTGGTCACTGCC	CCTTGCTGT**A**GGCATAGACCACAGAGCCCAGC
c.712A>G	p.Ile238Val	TGGTAC**G**TCGGCTTCCTTTGTCTCATCCTGGC	AGGAAGCCGA**C**GTACCAGGCAGTGACCAGCTCC
c.727C>T	p.Leu243Phe	TTCCTTTGT**T**TCATCCTGGCCTCGTTCCTGGTG	AGGATGA**A**ACAAAGGAAGCCGATGTACCAGGCAG
c.821C>T	p.Thr274Met	GGTGGGGCCTGATCA**T**GCTGACCACCA	TGGTGGTCAGC**A**TGATCAGGCCCCACC
c.827C>T	p.Thr276Ile	CGCTGA**T**CACCATTGGCTACGGGGACAAGTAC	GCCAATGGTG**A**TCAGCGTGATCAGGCCCCACC
c.826A>C	p.Thr276Pro	CACGCTG**C**CCACCATTGGCTACGGGGACAAG	CAATGGTGG**G**CAGCGTGATCAGGCCCCACCA
c.830C>T	p.Thr277Ile	TGACCA**T**CATTGGCTACGGGGACAAGTACCC	GTAGCCAATG**A**TGGTCAGCGTGATCAGGCCCC
c.833T>C	p.Ile278Thr	GACCACCA**C**TGGCTACGGGGACAAGTACCCC	CGTAGCCA**G**TGGTGGTCAGCGTGATCAGGCC
c.832A>G	p.Ile278Val	GACCACC**G**TTGGCTACGGGGACAAGTACCCC	CGTAGCCAA**C**GGTGGTCAGCGTGATCAGGCC
c.835G>T	p.Gly279Cys	ACCACCATT**T**GCTACGGGGACAAGTACCCCC	CCGTAGC**A**AATGGTGGTCAGCGTGATCAGGCC
c.836G>A	p.Gly279Ser	ACCACCATT**A**GCTACGGGGACAAGTACCCCC	CCGTAGC**T**AATGGTGGTCAGCGTGATCAGGCC
c.838T>C	p.Tyr280His	ACCATTGGC**C**ACGGGGACAAGTACCCCCAGAC	TCCCCGT**G**GCCAATGGTGGTCAGCGTGATCAG
c.841G>A	p.Gly281Arg	ATTGGCTAC**A**GGGACAAGTACCCCCAGACCTG	TTGTCCC**T**GTAGCCAATGGTGGTCAGCGTGATC
c.841G>T	p.Gly281Trp	ATTGGCTAC**T**GGGACAAGTACCCCCAGACCTG	TTGTCCC**A**GTAGCCAATGGTGGTCAGCGTGATC
c.846C>A	p.Asp282Glu	TACGGGGA**A**AAGTACCCCCAGACCTGGAACGG	GGGTACTT**T**TCCCCGTAGCCAATGGTGGTCAG
c.844G>C	p.Asp282His	CTACGGG**C**ACAAGTACCCCCAGACCTGGAACG	GGTACTTGT**G**CCCGTAGCCAATGGTGGTCAGC
c.851A>G	p.Tyr284Cys	GGGACAAGT**G**CCCCCAGACCTGGAACGGCAG	CTGGGGG**C**ACTTGTCCCCGTAGCCAATGGTGG
c.850T>G	p.Tyr284Asp	GGGGACAAG**G**ACCCCCAGACCTGGAACGGCA	TGGGGGT**C**CTTGTCCCCGTAGCCAATGGTGG
c.850T>C	p.Tyr284His	GGGGACAAG**C**ACCCCCAGACCTGGAACGGCA	TGGGGGT**G**CTTGTCCCCGTAGCCAATGGTGG

Table S2 - *continued*. **Sequence of mutagenic primers used to generate KCNQ2 variants.**

Nucleotide change	Amino acid change	Forward Primer	Reverse Primer
c.850T>A	p.Tyr284Asn	GGGGACAAG**A**ACCCCCAGACCTGGAACGGCA	TGGGGGT**T**CTTGTCCCCGTAGCCAATGGTGG
c.871A>G	p.Arg291Gly	ACCTGGAACGGC**G**GGCTCCTTGCGG	CCGCAAGGAGCC**C**GCCGTTCCAGGT
c.[875T>C:877C>T]	p.Leu292Pro:Leu293Phe	CAGGC**C**C**T**TTGCGGCAACCTTCACCCTCATCG	TTGCCGCAA**A**GGGCCTGCCGTTCCAGGTCTGGG
c.881C>T	p.Ala294Val	CTCCTTG**T**GGCAACCTTCACCCTCATCGGTG	AAGGTTGCC**A**CAAGGAGCCTGCCGTTCCAGG
c.881C>G	p.Ala294Gly	CTCCTTG**G**GGCAACCTTCACCCTCATCGGTG	AAGGTTGCC**C**CAAGGAGCCTGCCGTTCCAGG
c.913_915delTTC	p.Phe305del	TGTCTCCTTC**...**GCGCTGCCTGCAGGCATCTTG	CAGCGC**...**GAAGGAGACACCGATGAGGGTGAAG
c.916G>C	p.Ala306Pro	CTCCTTCTTC**C**CGCTGCCTGCAGGCATCTTGG	GCAGCG**G**GAAGAAGGAGACACCGATGAGGGTG
c.916G>A	p.Ala306Thr	CTCCTTCTTC**A**CGCTGCCTGCAGGCATCTTGG	GCAGCG**T**GAAGAAGGAGACACCGATGAGGGTG
c.917C>T	p.Ala306Val	CCTTCTTCG**T**GCTGCCTGCAGGCATCTTGGG	AGGCAGC**A**CGAAGAAGGAGACACCGATGAGGG
c.998G>A	p.Arg333Gln	GAGAAGAGGC**A**GAACCCGGCAGCAGGCCTGAT	GGGTTC**T**GCCTCTTCTCAAAGTGCTTCTGCCTG
c.997C>T	p.Arg333Trp	TTGAGAAGAGG**T**GGAACCCGGCAGCAGGCCTG	GTTCC**A**CCTCTTCTCAAAGTGCTTCTGCCTGTG
c.1004C>T	p.Pro335Leu	AGGCGGAACC**T**GGCAGCAGGCCTGATCCAGTC	GCTGCC**A**GGTTCCGCCTCTTCTCAAAGTGCTTC
c.1123C>G	p.Gln375Glu	TACAGTTCG**G**AAACTCAAACCTACGGGGCCTCC	GTTTGAGTTT**C**CGAACTGTACATGGGCACGGTG
c.1229C>T	p.Pro410Leu	AGGACCCCC**T**GCCGGAGCCGTCTCCAAGCC	CTCCGGC**A**GGGGGTCCTTCCTGAAAGCGAG
c.1505C>T	p.Ala502Val	GTGCCG**T**GTCACGGCAGAACTCAGAAGCAAGC	CTGCCGTGAC**A**CGGCACCCTTGATGCGGAAAGC
c.1545G>C	p.Glu515Asp	CGGAGA**C**GACATTGTGGATGACAAGAGCTGCCC	CCACAATGTC**G**TCTCCGGGGAGGCTTGCTTCTG
c.1627G>A	p.Val543Met	CAGAGCC**A**TGTGTGTCATGCGGTTCCTGGTGTC	TGACACACA**T**GGCTCTGATGCTGACTTTGAGGCC
c.1678C>T	p.Arg560Trp	GGAGAGCCTG**T**GGCCCTACGACGTGATGGACG	AGGGCC**A**CAGGCTCTCCTTGAACTTCCGCTTG
c.1700T>A	p.Val567Asp	ATGGACG**A**CATCGAGCAGTACTCAGCCGGC	TGCTCGATG**T**CGTCCATCACGTCGTAGGGCC
c.1732A>G	p.Met578Val	TGGAC**G**TGCTGTCCCGAATTAAGAGCCTGCAG	TCGGGACAGCA**C**GTCCAGGTGGCCGGCTGAGTA
c.1742G>A	p.Arg581Gln	TCCC**A**AATTAAGAGCCTGCAGTCCAGAGTGGAC	AGGCTCTTAATT**T**GGGACAGCATGTCCAGGTGGC
c.1757A>C	p.Gln586Pro	AGAGCCTGC**C**GTCCAGAGTGGACCAGATCGTGG	TCTGGAC**G**GCAGGCTCTTAATTCGGGACAGCATG
c.1764A>T	p.Arg588Ser	TGCAGTCCAG**T**GTGGACCAGATCGTGGGGCGG	GTCCAC**A**CTGGACTGCAGGCTCTTAATTCGGG
c.1810C>T	p.Arg604Cys	GGACAAGGAC**T**GCACCAAGGGCCCGGCCGAG	CCTTGGTGC**A**GTCCTTGTCCGTGATCGCTGG
c.1814C>G	p.Thr605Ser	AAGGACCGCA**G**CAAGGGCCCGGCCGAGGC	CCCTTG**C**TGCGGTCCTTGTCCGTGATCGC
c.1910T>G	p.Leu637Arg	AGAAGC**G**GGACTTCCTGGTGAATATCTACATGCAGC	CAGGAAGTCC**C**GCTTCTTCTCCATGGACAAGACCTGC
c.1988A>G	p.Glu663Gly	GGGGCCAAAG**G**GCCGGAGCCGGCGCCGCC	TCCGGC**C**CTTTGGCCCCAAAGTAGGCCTCG
c.2101_2103delTCT	p.Phe701del	CCAGAAGAAC**...**TCGGCGCCCCCGGCCGCG	CGCCGA**...**GTTCTTCTGGCCCGTGGAGCTG
c.2209G>A	p.Gly737Ser	GGACCAC**A**GCTCCCTGGTGCGCATCCCG	CCAGGGAGC**T**GTGGTCCCCCACGGGGGAG
c.2252C>T	p.Ser751L eu	CGAGCGGT**T**GCTGTCCGCCTACGGCGGG	CGGACAGC**A**ACCGCTCGTGGGCAGGCGG
c.2264A>G	p.Tyr755Cys	TGTCCGCCT**G**CGGCGGGGGCAACCGCGC	CCCGCCG**C**AGGCGGACAGCGACCGCTCG
c.2266G>A	p.Gly756Ser	TCCGCCTAC**A**GCGGGGGCAACCGCGCCA	CCCCCGC**T**GTAGGCGGACAGCGACCGCTC
c.2279G>A	p.Arg760His	GGCAACC**A**CGCCAGCATGGAGTTCCTGCG	ATGCTGGCG**T**GGTTGCCCCCGCCGTAGGC
c.2312C>T	p.Thr771Ile	CAGGAGGACA**T**CCCGGGCTGCAGGCCCCC	CCCGGG**A**TGTCCTCCTGCCGCAGGAACTC
c.2339A>C	p.Asn780Thr	AGGGGA**C**CCTGCGGGACAGCGACACGTC	GTCCCGCAGG**G**TCCCCTCGGGGGGCCTGC
c.2377G>C	p.Val793Leu	TCCCGTCC**C**TGGACCACGAGGAGCTGGAGC	GTGGTCCA**G**GGACGGGATGGAGATGGACGTG
c.2560C>T	p.Arg854Cys	CCCCGCCA**T**GCTCGGCCACCGGCGAGG	GGCCGAGC**A**TGGCGGGGGCCCGCACGG
c.2570C>T	p.Thr857Ile	CGGCCA**T**CGGCGAGGGTCCCTTTGGTGA	ACCCTCGCCG**A**TGGCCGAGCGTGGCGGGG
c.2572G>A	p.Gly858Ser	GCCACC**A**GCGAGGGTCCCTTTGGTGACG	GGACCCTCGC**T**GGTGGCCGAGCGTGGCGG

Table S3. Manual patch clamp and high throughput functional results.

See Excel file:

https://digitalhub.northwestern.edu/files/151bf778-d6be-49a9-b4b7-6f75ba9c0e2e

Table S4. Functional properties of CHO-Q3 cells electroporated with homozygous variant KCNQ2 cDNA recorded under control conditions.

See Excel file:

https://digitalhub.northwestern.edu/files/5e63c462-56c3-4cf5-9468-f4e2e20af714

Table S5. Functional properties of CHO-Q3 cells co-electroporated with heterozygous variant plus wild type KCNQ2 cDNA recorded under control conditions.

See Excel file:

https://digitalhub.northwestern.edu/files/33bd2d57-21b4-4d10-aa59-07e1d8551ada

Table S6 Functional properties of CHO-Q3 cells electroporated with homozygous variant KCNQ2 cDNA recorded following exposure to retigabine.

See Excel file:

https://digitalhub.northwestern.edu/files/ffb6d08c-4af6-41f9-b319-26b593987e01

Table S7. Functional properties of CHO-Q3 cells co-electroporated with heterozygous variant plus wild type KCNQ2 cDNA recorded following exposure to retigabine.

See Excel file:

https://digitalhub.northwestern.edu/files/b2c17941-0e0e-4255-b0fd-cf34f4628ea6